Parameter Sensitivity Analysis for A Thermal Coupling Simplified Electrochemical Model and Health Feature Extraction

Junfu Li, Dafang Wang, Qi Zhang, Jingwei Wang, Jinyi Cai, Zhihao Tang
School of Automotive Engineering
Harbin Institute of Technology
Wei Hai, China
lijunfu@hit.edu.cn

Lixin Wang
School of Mechanical Engineering and Automation
Harbin Institute of Technology
Shen Zhen, China
wlx@hit.edu.cn

***Abstract*—Battery state of health is critical for a battery management system because it can indicate how much energy can be effectively extracted. How to estimate SOH accurately becomes a big issue. This work develops a thermal coupling simplified electrochemical model that has good parameter identifiability. A sensitivity analysis is conducted to determine which parameters make more contributions on model simulation. The variations of battery terminal voltage and surface temperature caused by the changes of the parameters are used to assess their sensitivities. Then, an aging test is conducted to obtain the battery with different SOHs. Lastly, three sensitive parameters are selected as internal health features according to their correlation coefficients with SOH, which provides more health information for further SOH estimation.**

Keywords: Battery model; State of health; Sensitivity analysis; Internal health feature

I. INTRODUCTION

Li-ion batteries are popular because of their high working voltage, large energy density, low self-discharge rate, and no memory effect [1]. As an electrochemical power source fabricated from a variety of anode and cathode materials, battery's performance will degrade gradually due to the inevitable loss of li-ions and active materials. State of health (SOH) refers to the battery condition state compared to its initial condition, and is expressed as a loss of capacity relative to the initial value [2]. It determines how much energy can be maximumly extracted from the battery. Therefore, SOH estimation of li-ion batteries is critical for battery management systems (BMSs).

Battery performance continues to decline, which can be explained by a series of complex aging mechanisms. For examples, the SEI layer is formed on the carbon surface, and it continues to grow due to the continuous side reactions, which re-consumes li-ions and results in irreversible battery capacity loss and power reduction. Besides, pulverization of, or cracks and fractures in, the active materials due to intercalation process can also lead to battery capacity fade and power loss [2].

As the battery will degrade gradually, it is necessary to diagnose battery SOH to ensure safe and reliable use. The challenge in performing SOH estimation is that SOH can only be obtained via estimation in practical application of which the methods generally fail to meet the requirement in terms of the accuracy. Incremental capacity analysis (ICA) or differential voltage analysis (DVA) can indicate possible causes of the capacity decrease or the lithium-capacity-consuming side reactions, which are powerful analysis tools for battery health diagnosis [3,4]. However, the IC or DV charging data should be tested under small C rates. On the contrary, if larger current rate is applied during the experiment, smoothing methods need to be adopted to filter the noise on differential curves. It should be mentioned that the sampling frequency and the length of smoothing window also need to be taken into consideration [5]. Battery SOH can also be estimated based on external features (e.g. equivalent ohmic resistance, sample entropy) that are extracted from external characteristic curves. However, the accuracy of SOH estimation cannot be well ensured due to casual sampling frequency and variable operating conditions.

A battery model with degradation physics is very helpful in SOH estimation, because it can simulate battery external characteristics under complex operating working conditions at different aging stages. The models that have been mainly used in the past are equivalent circuit models (ECMs) [6,7]. ECMs consist of a few electronic components (e.g., resistance, capacitance, and inductance) and have simple structures, but their accuracy under constant charge and discharge rates is insufficient. Besides, their parameters need to be updated frequently because they change over with SOH, state of charge, current and temperature. Thus, ECMs are not proper for SOH estimation.

By comparison, electrochemical models (e.g., Pseudo 2-dimensional models and their derivatives) [8-10] which are based on theories of porous electrodes and concentrated solutions can more accurately simulate both external characteristics (e.g., terminal voltage and surface temperature) and internal states (e.g., overpotential and liquid-phase lithium-ion concentration). They generally have many parameters to be identified. Some parameters, like the length and the weight of

1.Program of Shenzhen knowledge innovation (JCYJ20180306171803050)
2.Fundamental Research Funds for the Central Universities (HIT.NSRIF.201705)

978-1-7281-0860-5/19/$31.00 ©2019 IEEE

the battery, can be directly measured or provided by the manufacturers. Some need electrochemical measurements, which even require the dismantling of the cell into components. The others parameters such as the radius of the particle need to be identified through estimation algorithms (e.g. genetic algorithm and particle swarm optimization) [11]. However, an estimation algorithm generally fails to ensure the accuracy of all the parameters. With model simplification and parameter regroup, physical parameters such as diffusion coefficient or liquid-phase conductivity can be transformed into model parameters that can be identified individually with the excitation response analysis [12]. As model parameters have similar physical meanings, their changing laws can indicate a battery's health state. Due to the above advantages, electrochemical models are becoming more and more attractive in recent years in BMSs especially for SOH estimation.

This work introduces a thermal coupling simplified electrochemical (TC-SFP) model. A parameter sensitivity analysis is then conducted to determine which parameters make more contribution on the battery performances. Internal health features are selected according to the correlation coefficients between model sensitive parameters and battery SOH.

II. BATTERY MODEL AND MODEL PARAMETER

A simplified first principle (SFP) model was developed based on a single particle model which assumed the chemical reaction on the active particles in the thickness direction of each electrode to be uniform. The characteristics of the electrodes could be represented by two single spherical particles. This model could describe the physiochemical processes (e.g., solid-phase diffusion, chemical reaction, liquid-phase diffusion) inside the battery. A simplified thermal resistance model was coupled with the SFP model to calculate the internal average temperature T and surface temperature T_{surf}. The primary parts of the TC-SFP model is shown in Table I. Model parameters that need to be identified are listed in Table II. The model parameter identification method can be found in our previous work [12].

TABLE I. THE PRIMARY PARTS OF THE TC-SFP MODEL

Physic	TC-SFP model
Terminal voltage	$U_{app}(t)=E_{ocv}(t)-\eta_{con}(t)-\eta_{act}(t)-\eta_{ohm}(t)$
Nernst equation	$E_{ocv}(t)=E_{ocv}^{ref}(t)+(T(t)-T_{ref})\dfrac{\mathrm{d}E_{ocv}(t)}{\mathrm{d}T}$
Basic working process	$E_{ocv}^{ref}(t)=U_p(y_{surf}(t))-U_n(x_{surf}(t))$ $y_{avg}(t)=y_0+I(t)t/Q_p \quad x_{avg}(t)=x_0-I(t)t/Q_n$
Solid-phase diffusion	$y_{surf}(t)=y_{avg}(t)+\Delta y(t) \quad x_{surf}(t)=x_{avg}(t)-\Delta x(t)$ $\Delta y(t)=\Delta y_1(t)+\dfrac{2}{7}\dfrac{\tau_p(t)}{Q_p}I(t) \quad \Delta x(t)=\Delta x_1(t)+\dfrac{2}{7}\dfrac{\tau_n(t)}{Q_n}I(t)$ $\Delta y_1(t_{k+1})=\Delta y_1(t_k)+\dfrac{1}{\tau_p(t)}(\dfrac{12}{7}\dfrac{\tau_p(t)}{Q_p}I(t_k)-\Delta y_1(t_k))(t_{k+1}-t_k)$ $\Delta x_1(t_{k+1})=\Delta x_1(t_k)+\dfrac{1}{\tau_n(t)}(\dfrac{12}{7}\dfrac{\tau_n(t)}{Q_n}I(t_k)-\Delta x_1(t_k))(t_{k+1}-t_k)$
Reaction polarization	$\eta_{con}(t)=\dfrac{2RT(t)}{F}(1-t_+)\ln(\dfrac{c_0+\Delta c(t)}{c_0-\Delta c(t)})$ $\Delta c(t_{k+1})=\Delta c(t_k)+\dfrac{1}{\tau_e}(P_{con}(t)I(t_k)-\Delta c(t_k))(t_{k+1}-t_k)$
Ohmic polarization	$\eta_{act}(t)=\dfrac{2RT(t)}{F}(\ln(\sqrt{m_n^2(t)+1}+m_n(t))+\ln(\sqrt{m_p^2(t)+1}+m_p(t)))$ $m_p(t)=\dfrac{1}{6Q_pc_0^{0.5}}\dfrac{1}{(1-y_{surf}(t))^{0.5}(y_{surf}(t))^{0.5}}P_{act}(t)I(t)$ $m_n(t)=\dfrac{1}{6Q_nc_0^{0.5}}\dfrac{1}{(1-x_{surf}(t))^{0.5}(x_{surf}(t))^{0.5}}P_{act}(t)I(t)$
Heat generation	$\eta_{ohm}(t)=R_{ohm}(t)I(t)$
Thermal calculation	$G(t)=I(t)(\eta_{con}(t)+\eta_{act}(t)+\eta_{ohm}(t)-T(t)\dfrac{\mathrm{d}E_{ocv}(t)}{\mathrm{d}T})$
Empirical behaviors	$T(t_k)=T(t_{k-1})+(t_k-t_{k-1})(G(t_{k-1})-\dfrac{T(t_{k-1})-T_{surf}(t_{k-1})}{R_{cond}})\dfrac{1}{m_{roll}C_p}$ $T_{surf}(t_k)=\dfrac{T_{surf}(t_{k-1})m_{can}C_{can}R_{cond}+(t_k-t_{k-1})(T(t_k)+R_{cond}A_0hT_a(t_k))}{m_{can}C_{can}R_{cond}+(t_k-t_{k-1})+R_{cond}(t_k-t_{k-1})A_0h}$
	$R_{ohm}(t)=R_{ohm}^{ref}\exp(\lambda_{ohm}(1/T_{ref}-1/T(t)))$ $P_{act}(t)=P_{act}^{ref}\exp(\lambda_{act}(1/T_{ref}-1/T(t)))$ $P_{con}(t)=P_{con}^{ref}\exp(\lambda_{con}(1/T_{ref}-1/T(t)))$ $\tau_p(t)=\tau_p^{ref}\exp(\lambda_{\tau p}(1/T_{ref}-1/T(t)))$ $\tau_n(t)=\tau_n^{ref}\exp(\lambda_{\tau n}(1/T_{ref}-1/T(t)))$

TABLE II. DEFINITIONS OF TC-SFP MODEL PARAMETERS

Parameters	Values
y_0 (–)	0.7998
x_0 (–)	0.4509
Q_p (A s)	6.1971×10^3
Q_n (A s)	3.5911×10^3
τ_p^{ref} (s)	0.0652
$\lambda_{\tau p}$ (K)	–208.4819
τ_n^{ref} (s)	2.9012×10^5
$\lambda_{\tau n}$ (K)	-4.6954×10^3
P_{act}^{ref} ($\mathrm{m^{-1.5}\ mol^{0.5}\ s}$)	113.97
λ_{act} (K)	-3.1036×10^3
P_{con}^{ref} ($\mathrm{mol\ m^{-3}\ A^{-1}}$)	21.78
λ_{con} (K)	-1.0773×10^3
τ_e (s)	1.0038×10^3
R_{ohm}^{ref} (Ω)	–633.18
λ_{ohm} (K)	60.40
R_{cond} ($\mathrm{K\ W^{-1}}$)	1.1392
h ($\mathrm{W\ m^{-2}\ K^{-1}}$)	25.01

III. MODEL PARAMETER SENSITIVITY ANALYSIS

Model parameters are independent with temperature and C rates, but related to battery SOH. To assess the contributions of each parameter on model simulation, parameter sensitive

analysis is first conducted to determine which parameters have larger effects.

17 parameters required assessments through sensitivity analysis. Its detailed implementations are as follows: for a certain parameter, 10 values at range of ±10% with 2% intervals are firstly obtained separately. Battery behaviors are then simulated using these 10 values. With no parameter changed, the average and maximum errors of T_{surf} are 0.5334 and 1.2691 °C, respectively, and the average and maximum errors of U_{app} are 20.74 and 590.73 mV, respectively. It is worth mentioning that when an individual parameter is investigated, the other parameters remain unchanged.

The variations of U_{app} and T_{surf} caused by the changes of model parameters are used to assess their sensitivities, which is defined as the standard deviation compared with no parameter changed. The operating conditions used for sensitivity analysis are under 25 °C at 0.5 C rate. The sensitivity of each parameter is listed in Table III.

TABLE III. STANDARD DEVIATIONS FOR MODEL PARAMETERS

Parameters	T_{surf} average	T_{surf} max	U_{app} average	U_{app} max
x_0	0.0068	0.022	4.13	210.78
y_0	0.079	0.095	39.80	406.97
Q_p	0.080	0.053	23.54	410.85
Q_n	0.0037	0.010	8.72	235.53
R_{ohm}^{ref}	0.0092	0.010	1.31	1.58
λ_{ohm}	4.72×10^{-5}	8.31×10^{-6}	0.0059	0.016
P_{act}^{ref}	0.010	0.010	1.53	3.74
λ_{act}	5.71×10^{-4}	3.26×10^{-5}	0.098	0.45
τ_p^{ref}	1.18×10^{-4}	9.46×10^{-5}	0.027	0.015
$\lambda_{\tau p}$	3.11×10^{-5}	1.39×10^{-5}	9.30×10^{-4}	0.0073
τ_n^{ref}	5.28×10^{-4}	5.33×10^{-5}	0.50	20.99
$\lambda_{\tau n}$	3.43×10^{-5}	7.96×10^{-6}	0.016	0.77
P_{con}^{ref}	4.10×10^{-4}	4.8×10^{-4}	0.058	0.065
λ_{con}	3.95×10^{-5}	9.05×10^{-6}	0.0041	0.012
τ_e	6.81×10^{-5}	1.98×10^{-5}	0.012	0.0073
h	0.050	0.0019	0.092	1.05
R_{cond}	7.44×10^{-5}	6.80×10^{-4}	0.0052	0.060

To assess the influences of the parameters on simulation results, model parameters can be categorized into two classes: sensitivity parameters (highlighted in bold) and insensitive parameters. A typical cluster of curves with different values of a certain parameter y_0 are shown in Fig. 1. It can be seen from Table III that the standard deviations of parameter y_0 are the largest. The reason that can explain such phenomenon is that y_0 determines the positions of the cut-off voltage and the platform of the terminal voltage. Without an accurate identification of y_0, battery simulation results will be much influenced.

The changes of other parameters, like x_0, Q_p, and Q_n, also affluence battery performance in terms of T_{surf} and U_{app}. Parameters R_{ohm}^{ref}, P_{act}^{ref}, τ_n^{ref}, and h are relatively lower-sensitivity parameters, because their changes just affluence battery simulation of U_{app}. As for the other parameters, their changes have little influence on simulation accuracy. Considering sensitivities of different parameters, sensitive parameters are y_0, x_0, Q_p, Q_n, R_{ohm}^{ref}, P_{act}^{ref}, τ_n^{ref}, and h.

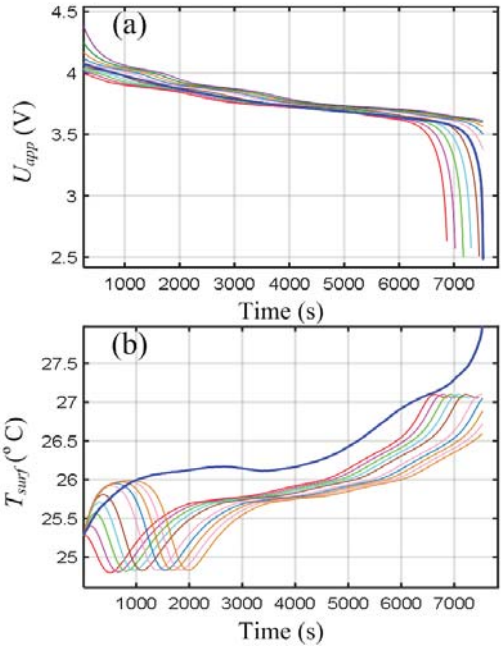

Figure 1. The cluster of curves with different values of y_0

It should be mentioned that as for the heat transfer coefficient h, it is determined by the heat dissipation conditions (e.g., the air velocity and battery surface area exposed to the air), and it has nothing to do with the property of the battery itself. Besides, a battery's ohmic resistance cannot be easily measured. For batteries with $LiFePO_4$ positive materials, its value is less than 10 mΩ. Thus, R_{ohm}^{ref} as well as h can be regarded as fixed during the battery lifetime.

IV. INTERNAL HEALTH FEATURE EXTRACTION

In this part, an aging test is conducted and model parameters are identified at different SOHs. The schedule of the aging test is shown in Fig. 2. The identification results at different cycles are shown in Table IV. The variation laws of the above sensitive parameters as well as a theoretical capacity Q_{all} are shown in Figs. 3-9.

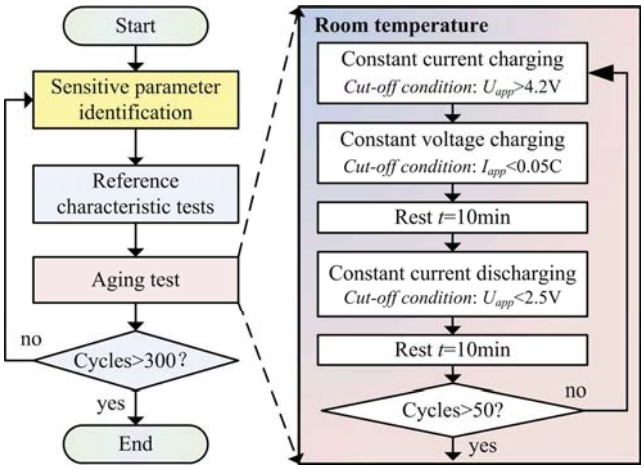

Figure 2. Schedule of aging test

TABLE IV. IDENTIFICATION RESULTS OF SENSITIVE PARAMETER

Cycle	**1**	**50**	**100**	**150**
x_0	0.4505	0.4443	0.4521	0.4576
y_0	0.8125	0.6761	0.6500	0.6656
Q_p	5.8336×10^3	5.7304×10^3	5.4476×10^3	5.1407×10^3
Q_n	3.5816×10^3	3.8992×10^3	3.8769×10^3	3.629×10^3
P_{act}^{ref}	2.6261×10^3	2.6423×10^3	1.8499×10^3	1.8875×10^3
τ_n^{ref}	13.33	74.72	131.00	177.91
Cycle	**200**	**250**	**300**	
x_0	0.4588	0.4497	0.4605	
y_0	0.6448	0.6132	0.6267	
Q_p	4.8193×10^3	4.1057×10^3	4.4410×10^3	
Q_n	3.6182×10^3	3.7042×10^3	3.4476×10^3	
P_{act}^{ref}	2.6761×10^3	1.8889×10^3	2.3381×10^3	
τ_n^{ref}	189.15	229.89	202.85	

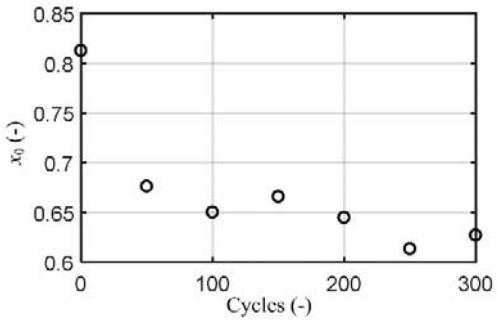

Figure 3. Variation laws of parameter x_0

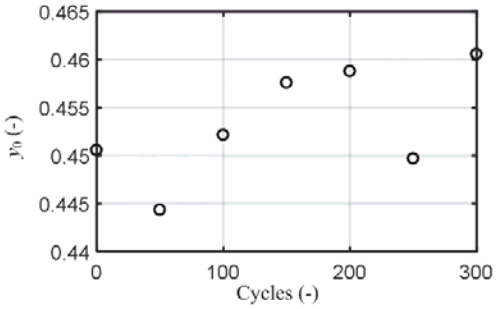

Figure 4. Variation laws of parameter y_0

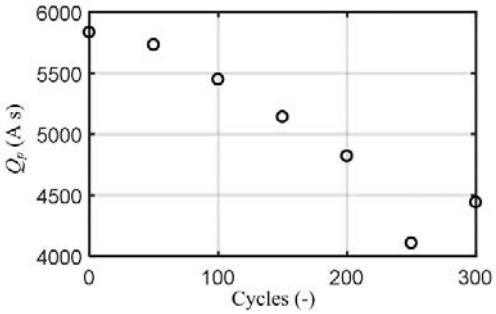

Figure 5. Variation laws of parameter Q_p

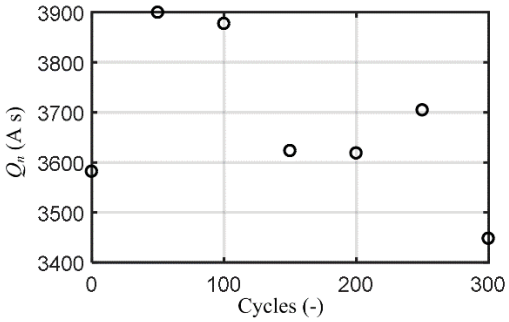

Figure 6. Variation laws of parameter Q_n

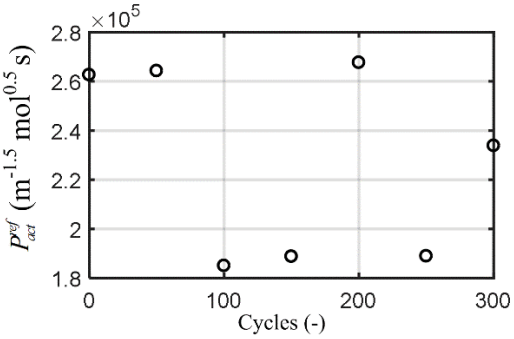

Figure 7. Variation laws of parameter P_{act}^{ref}

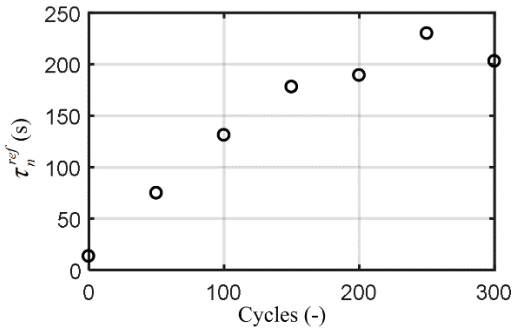

Figure 8. Variation laws of parameter τ_n^{ref}

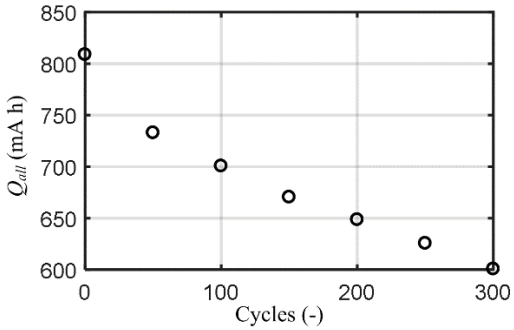

Figure 9. Variation laws of parameter Q_{all}

It can be seen from Fig. 3 that parameter x_0 decreased over cycles which followed the form of power exponential. However, there is no obvious trend for parameter y_0 and it just fluctuated around 0.45 with the amplitude less than 0.01. The variation law of Q_p shown in Fig. 5 generally followed a linear form except for the value identified at cycle 250, while the variation law of Q_n was not obvious. The reaction polarization coefficient P_{act}^{ref} shown in Fig. 7 had a large amplitude of fluctuations, and the variation law of τ_n^{ref} shows an increasing trend which is shown in Fig. 8. In addition, the variation law of Q_{all} is also shown in Fig. 9. Like Q_p, it showed a linear decreasing trend during the whole life cycle.

In order to select the potential internal features to indicate battery SOH, a correlation analysis is conducted and the correlation coefficients between capacity Q_{all} and the other sensitive parameters are shown in Table V.

TABLE V. CORRELATION COEFFICIENTS

Parameter	Correlation coefficient
x_0	0.9083
y_0	–0.5849
Q_p	0.9043
Q_n	0.3285
P_{act}^{ref}	0.3827
τ_n^{ref}	–0.9691

As is seen from Table V, the correlation coefficients of x_0, Q_p, and τ_n^{ref} are beyond 0.9, which means that they change over with SOH. x_0, Q_p, and τ_n^{ref} can thus be selected as internal health indicators. With a long-term monitoring of these three parameters' changing laws, SOH can be estimated or predicted, which leaves us much room for future work.

V. CONCLUSION

This work introduced a thermal coupling simplified electrochemical model and conducted a parameter sensitivity analysis to determine sensitive parameters. Three parameters x_0, Q_p, and τ_n^{ref} are selected as internal health features to indicate battery SOH. The main contributions of this work are as follows: (1) it provides accurate battery health information through analyzing the changing laws of health features, and (2) it provides more useful features for battery screening, which ensures the consistency of battery pack.

ACKNOWLEDGMENT

We thank the financial support by the program of Shenzhen knowledge innovation (20180213233441046). This work was also financially supported by the Fundamental Research Funds for the Central Universities (HIT.NSRIF.201705).

REFERENCES

[1] X. Hu, S. Li, and H. Peng, "A comparative study of equivalent circuit models for Li-ion batteries," Journal of Power Sources, vol. 198, pp. 359-367, 2012.

[2] J. Li, K. Adewuyi, N. Lotfi, R. G. Landers, and J. Park, "A single particle model with chemical/mechanical degradation physics for lithium ion battery State of Health (SOH) estimation," Applied Energy, vol. 212, pp. 1178-1190, 2018.

[3] M. Dubarry, V. Svoboda, R. Hwu, and B. Y. Liaw, "Capacity and power fading mechanism identification from a commercial cell evaluation," Journal of Power Sources, vol. 165, no. 2, pp. 566-572, 2007.

[4] M. Dubarry, and B. Y. Liaw, "Development of a universal modeling tool for rechargeable lithium batteries," Journal of Power Sources, vol. 174, no. 2, pp. 856-860, 2007.

[5] X. Tang, C. Zou, K. Yao, G. Chen, B. Liu, Z. He, and F. Gao, "A fast estimation algorithm for lithium-ion battery state of health," Journal of Power Sources, vol. 396, pp. 453-458, 2018.

[6] L. Zhu, Z. Sun, H. Dai, and X. Wei, "A novel modeling methodology of open circuit voltage hysteresis for LiFePO 4 batteries based on an adaptive discrete Preisach model," Applied Energy, vol. 155, pp. 91-109, 2015.

[7] G. Dong, J. Wei, Z. Chen, H. Sun, and X. Yu, "Remaining dischargeable time prediction for lithium-ion batteries using unscented Kalman filter," Journal of Power Sources, vol. 364, pp. 316-327, 2017.

[8] T. F. Fuller, M. Doyle, and J. Newman, "RELAXATION PHENOMENA IN LITHIUM-ION-INSERTION CELLS," Journal of The Electrochemical Society, vol. 141, no. 4, pp. 982-990, 1994.

[9] M. Doyle, J. Newman, A. S. Gozdz, C. N. Schmutz, and J. M. Tarascon, "Comparison of modeling predictions with experimental data from plastic lithium ion cells," Journal of The Electrochemical Society, vol. 143, no. 6, pp. 1890-1903, 1996.

[10] S. K. Rahimian, S. Rayman, and R. E. White, "Comparison of single particle and equivalent circuit analog models for a lithium-ion cell," Journal of Power Sources, vol. 196, no. 20, pp. 8450-8462, 2011.

[11] L. Zhang, L. Wang, G. Hinds, C. Lyu, J. Zheng, and J. Li, "Multi-objective optimization of lithium-ion battery model using genetic

algorithm approach," Journal of Power Sources, vol. 270, pp. 367-378, 2014.

[12] J. Li, L. Wang, C. Lyu, H. Wang, and X. Liu, "New method for parameter estimation of an electrochemical-thermal coupling model for $LiCoO_2$ battery," Journal of Power Sources, vol. 307, pp. 220-230, 2016.